Crystallinity, Conductivity, and Magnetic Properties of PVDF-Fe_3O_4 Composite Films

Aarti S. Bhatt, D. Krishna Bhat, M. S. Santosh

Department of Chemistry, National Institute of Technology, Karnataka 575025, India

Received 16 January 2010; accepted 12 May 2010
DOI 10.1002/app.32796
Published online 29 July 2010 in Wiley Online Library (wileyonlinelibrary.com).

ABSTRACT: The formation of Fe_3O_4 nanoparticles by hydrothermal process has been studied. X-ray Diffraction measurements were carried out to distinguish between the phases formed during the synthesis. Using the synthesized Fe_3O_4 nanoparticles, poly(vinyledene fluoride)-Fe_3O_4 composite films were prepared by spin coating method. Scanning electron microscopy of the composite films showed the presence of Fe_3O_4 nanoparticles in the form of aggregates on the surface and inside of the porous polymer matrix. Differential Scanning calorimetry revealed that the crystallinity of PVDF decreased with the addition of Fe_3O_4. The conductitivity of the composite films was strongly influenced by the Fe_3O_4 content; conductivity increased with increase in Fe_3O_4 content. Vibration sample magnetometry results revealed the ferromagnetic behavior of the synthesized iron oxide nanoparticles with a Ms value of 74.50 emu/g. Also the presence of Fe_3O_4 nanoparticles rendered the composite films magnetic. © 2010 Wiley Periodicals, Inc. J Appl Polym Sci 119: 968–972, 2011

Key words: nanocomposites; PVDF; crystallinity; conductivity; magnetization

INTRODUCTION

Magnetic nanomaterial has recently become one of the most active research fields in the areas of chemistry and engineering. This is mainly because nanomaterials display novel and often enhanced properties compared with traditional materials, which open up possibilities for new technological applications. Among the nanosized metal oxides, iron oxides have become of long standing interest, because of its rich variety of applications in electronic, magnetic, optical, and mechanical devices.[1,2]

PVDF is a polycrystalline polymer that started drawing scientific interest in the 70s, because of its extraordinary piezoelectric properties. Yan et al. have prepared organic-inorganic composite membranes by dispersing nanosized alumina particles in the PVDF solution by phase inversion process.[3] Moreover, an increasing interest has been devoted to PVDF as electric and/or magnetic field sensors. Electrical and gas sensing properties of Li and Ti codoped NiO (LTNO)/PVDF nanocomposites were investigated wherein LTNO with a composition of $Li_{0.1}Ti_{0.018}Ni_{0.882}O$ was prepared using citrate – gel technique.[4] For electrical and magnetic applications, fillers such as metal oxides and ferrites are used to provide better electrical and magnetic properties. Polymer based composites with high dielectric constant or high initial permeability have attracted much attention, because of their flexibility, compatibility with print-wiring-board, and ability to be easily fabricated into various shapes. The high initial permeability is mainly obtained by dispersing ferrite particles with large initial permeability into the polymer matrix.[5–7] Also, addition of nanoscale magnetite particles improves the magnetic properties of the otherwise non magnetic polymer. Xu et al.[8] have prepared PVDF/Fe_3O_4 nanocomposites by coprecipitation method and have studied their magnetic and optical behaviors. However, thermal and conductivity properties of these nanocomposites were not considered.

In this work, we have prepared Fe_3O_4 nanoparticles dispersed PVDF nanocomposite films by a simple ultrasonication method. The focus of this work has been to study the crystallinity and conductivity of the composite films after the addition of nanoparticles alongwith their magnetic behavior.

EXPERIMENTAL

Materials

The starting materials for the preparation of iron oxide powders were ferric chloride, ($FeCl_3.6H_2O$) and hydrazine hydrate 99% (both of analytical grade). Distilled water was used throughout the experiment. PVDF (M_w = 275,000) was used in the pellet form.

Correspondence to: D. K. Bhat (denthajekb@gmail.com).

Synthesis of iron oxide powder by hydrothermal process

For the hydrothermal synthesis of iron oxide, high temperature and pressure maintaining apparatus, that is, "autoclave" or "bomb" was used. Known amount of iron salt was taken in a beaker and dissolved by adding few drops of dilute HCl followed by 10 mL of distilled water. The solution was then stirred for 30 min to make it homogeneous. Known amount of hydrazine hydrate was added and again stirred for 1 h, to ensure proper mixing of the reagents. The solution was then transferred to the bomb, which was kept in oven at 473 K for different durations. The precipitate obtained was centrifuged several times by giving alternate wash with ethanol and water. The precipitate was finally dried in an oven maintained at 333 K.

Preparation of PVDF-Fe_3O_4 nanocomposite film

PVDF was dissolved in DMF to obtain a 40% solution (w/v). To this PVDF solution synthesized iron oxide magnetic particles (prepared by heating at 473 K for 5 h) at 3 different weight ratios were added. The solutions were then heated on a water bath at 363 K for 5 h, till the solution became completely homogeneous. According to the weight ratios of oxide added, the resulting composites were termed as PF1 = 1 wt %, PF2 = 3 wt %, and PF3 = 5 wt %. Each PVDF-iron oxide suspensions were spin coated on a glass substrate at 500 rpm, 1000 rpm, and 2000 rpm for 60 s sequentially (Spin coater ACE-1020 Series). The glass substrate was then immersed in distilled water for 12 h to finally get the PVDF-Fe_3O_4 films.

Under similar conditions, undoped PVDF film was also prepared and termed PF0

The X-ray powder diffraction analysis was conducted on a Bruker ASS X –Ray Diffractometer at a scanning rate of 4° per minute with 2Θ ranging from 10° to 90°, using Cu Kά radiation (λ = 1.5406 Å). Scanning Electron Microscope was used for morphological and microchemical analysis (JASCO). Differential Scanning Calorimetry (DSC) data was obtained in the temperature range of 35–250°C (DSC-60, Shimadju, Japan). The samples were heated at a rate of 10°C per minute in Nitrogen atmosphere. The samples were sealed in an aluminum pan. An empty pan was used as reference. The electric properties of the films were measured by four probe method using KEITHLEY 2182A. The magnetic properties were assessed with a Vibration Sample Magnetometer (ADE–DMS EV -7VSM). From the magnetic saturation and coercivity values, the effect of the nanoparticles was evaluated.

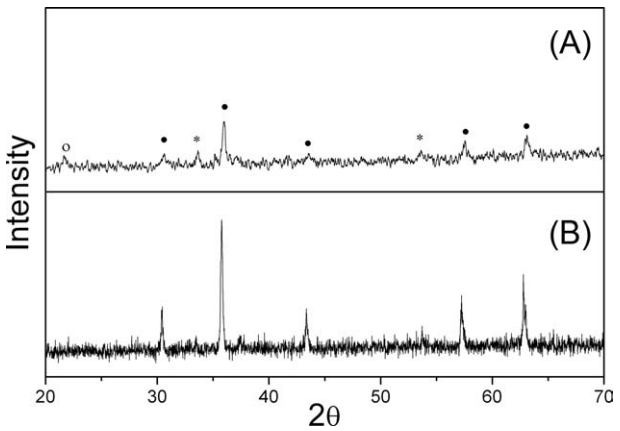

Figure 1 XRD pattern of iron oxide particles synthesized at 473 K for (A) 5 h (B) 1 h (• = Fe_3O_4, * = α-Fe_2O_3, o = α-FeOOH).

RESULTS AND DISCUSSION

X-ray diffraction (XRD) analysis

Structure and phase purity of the samples were investigated by XRD. Figure 1(A,B) show the XRD pattern of the samples prepared by heating at 473K for 5 h and 1 h, respectively. Figure 1(B) shows mixture of α-FeOOH, α-Fe_2O_3, and Fe_3O_4. By increasing the duration of heating to 5 h, the intensity of peaks corresponding to Fe_3O_4 increased showing a better crystallinity [Fig. 1(A)]. Heating the sample for 7 h also showed the same result. This shows that higher reaction duration was necessary for the formation of Fe_3O_4 nanoparticles. The major diffraction peaks at 2Θ = 30.1°, 35.5°, 43.0°, 57.7°, and 62.7° can be indexed to (220), (311), (400), (511), and (400) planes of magnetite, respectively. These reflection peaks correspond to the standard file JCPDS no. 82–1533, indicating the sample has a cubic crystalline structure.

Scanning electron microscopy (SEM) analysis

SEM analysis provides information on the size and morphology of the products. Figure 2 shows the SEM micrograph of the synthesized iron oxide particles. One can see Fe_3O_4 nanoparticles with sizes in the range 60–80 nm forming large agglomerates and relatively wide size distribution. Most of these Fe_3O_4 nanoparticles have irregular shapes and a few have hexagonal shape. It is known that the uniformity of size and shape is controlled by nucleation.[9] After hydrazine was rapidly added at room temperature the reaction started. The nucleation and crystal growth continued during heating, which may result in the wide size distribution and irregular shape of Fe_3O_4 nanoparticles.

Figure 3(A–D) presents SEM images of the surfaces of the PF0, PF1, PF2, and PF3 films. The images

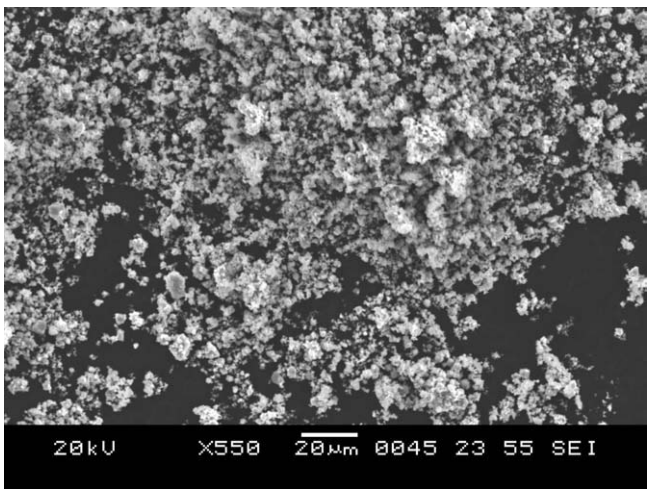

Figure 2 SEM micrograph of the synthesized iron oxide particles.

reveal a porous sponge like structure with aggregations of Fe_3O_4 nanoparticles appearing clearly on the surface and inside the pores. Although a uniform distribution of the nanoparticles in the polymer matrix was aimed, the aggregation of the Fe_3O_4 nanoparticles in the PVDF matrix was not prohibited because of the aggregation interaction.

DSC analysis

The thermal behavior and crystallinity of the films have been examined by DSC, and the results are shown in Figure 4. It was observed that all the films exhibit a main melting peak around 165°C at the scanning rate of 10°C per minute. The heat of fusion for PF0, PF1, PF2, and PF3 is 75.14, 58.91, 45.01, and 44.59 J/g, respectively. By assuming that pure PVDF was 100% crystalline, the relative percentage of crystalline was calculated based on eq. (1) given below:

$$\% \text{ crystallinity} = (\Delta H/\Delta H^0) \times 100 \quad (1)$$

where ΔH^0 is the heat of fusion of pure PVDF(105 J/g)[10] and ΔH is related to the PVDF-Fe_3O_4 composites.[11] The results, presented in Table I, show a decrease in crystallinity with increase in magnetite content. This is in line with the results obtained by Xu et al.[8] This may have resulted from the partial inhibition effect of Fe_3O_4 addition on polymer crystal formation, just as the inorganic fillers such as α-Al_2O_3, TiO_2, γ-$LiAlO_2$, and Sm_2O_3 decreased the crystalline phase of PEO-based polymer electrolyte system.[12–16] Also, some kind of interactions between iron, oxygen in Fe_3O_4, and fluorine in PVDF may occur, which not only induces structural modification of the polymer

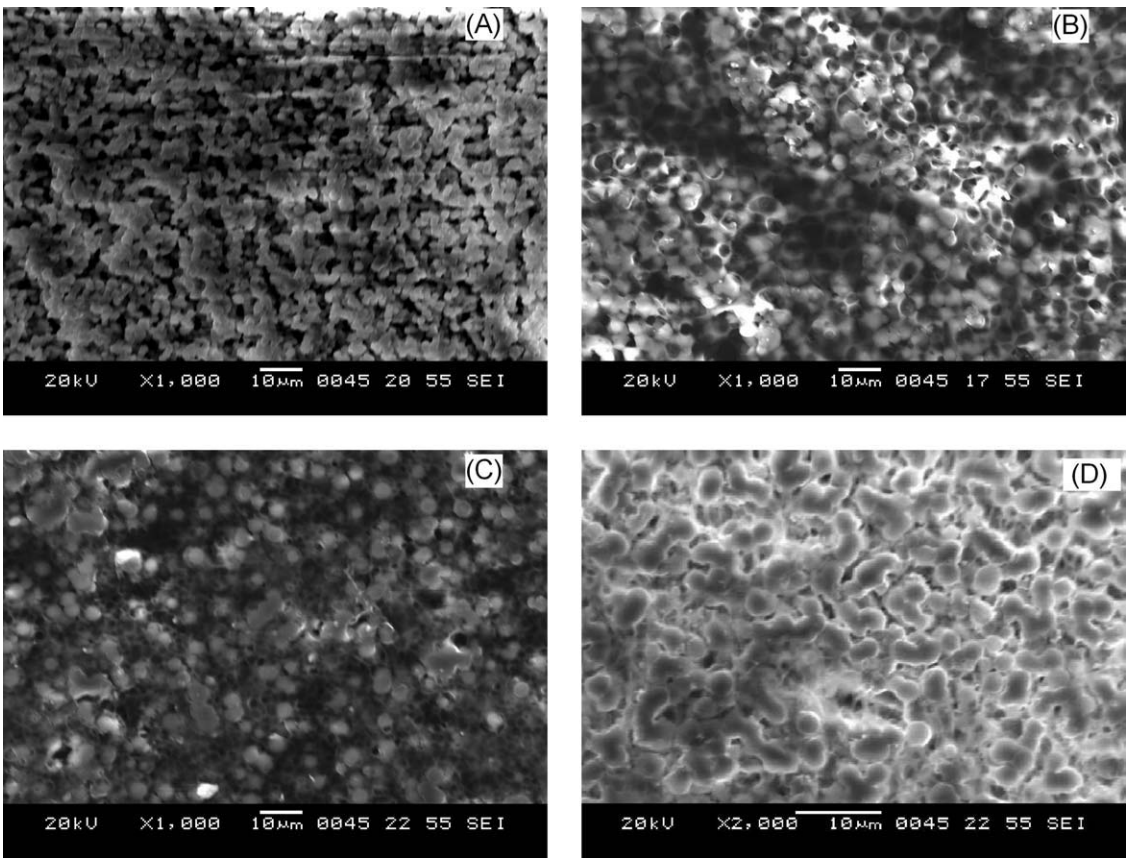

Figure 3 SEM micrographs (A) PF0, (B) PF1, (C) PF2, and (D) PF3.

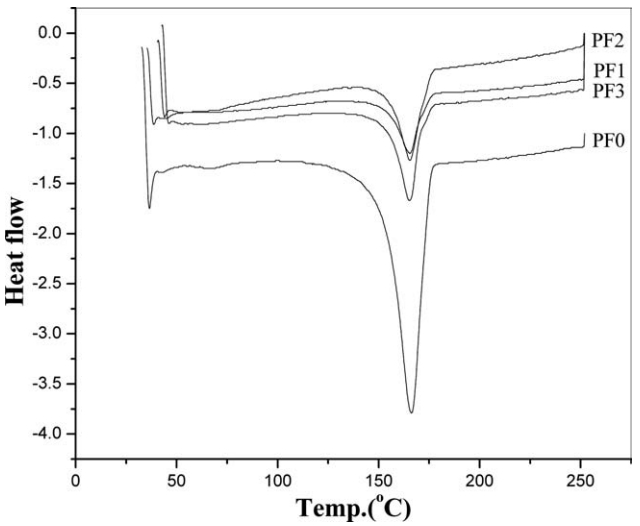

Figure 4 DSC of the PVDF and iron oxide-PVDF composite films.

chain, but also favors improvement of the conductivity,[11,17] as was further demonstrated by the conductivity measurement results in the next section.

Conductivity studies

Table II displays the room temperature conductivity and resistivity for the composite films. As mentioned in section 3.3, the nanosized Fe_3O_4 particles can interact with PVDF. On one hand, the interaction of Fe_3O_4 nanoparicles with PVDF segments results in the structural modification of the polymer chain, thereby favoring the conductivity. However, the interaction of Fe_3O_4 and PVDF decreases the crystalline phase in the polymer, as seen in the thermal studies. The restriction of crystallization and the increase of amorphous phase favor the improvement of ionic mobility and conductivity also.[18] Y.J. Wang and D. Kim[11] strongly related ionic conductivity in the PVDF/LiClO4/TiO2 system to the nanosized TiO2 content; wherein the conductivity initially increased but then decreased with further increasing TiO2 content. However, in this study, with the Fe_3O_4 content at 1 wt % in the PVDF-magnetite system, the conductivity remains constant with that of the PVDF system without Fe_3O_4. However, the conductivity increased for the PVDF-magnetite system

TABLE I
Enthalpy and % crystallinity Values of the Composite Films

Sample	Enthalpy (J/g)	Crystallinity (%)
PF 0	71.54	100.00
PF 1	58.91	56.10
PF 2	45.01	42.87
PF 3	44.59	42.47

TABLE II
Resistance and Conductance Values of the Composite Films at Room Temperature

Sample	Resistivity (ohm cm)	Conductivity (S/cm)
PVDF	0.175	5.70
1%	0.175	5.70
3%	0.166	6.03
5%	0.153	6.52

with 3 wt % and 5 wt % Fe_3O_4 content (6.03 S/cm and 6.52 S/cm, respectively). A composite film with higher Fe_3O_4 content was not feasible because, when the content of Fe_3O_4 exceeded 5 wt %, it became almost impossible to obtain the PVDF-Fe_3O_4 film.

Magnetic measurements

The room temperature magnetization curves of Fe_3O_4 nanoparticles and composite films are presented in Figure 5(A,B), respectively. From the magnetization curves, the magnetic properties, the

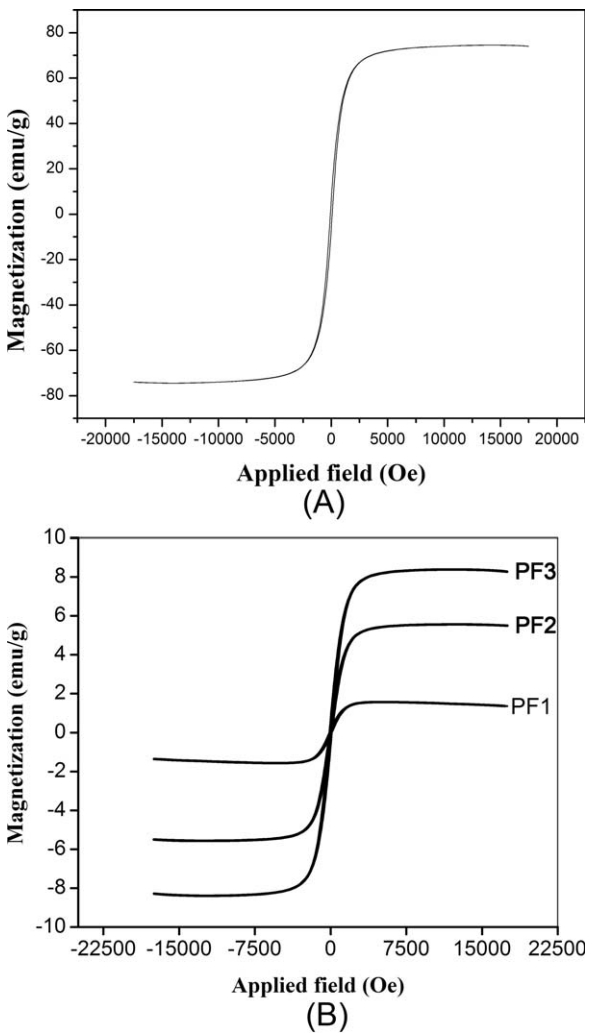

Figure 5 Room temperature magnetization curves (A) Fe_3O_4 nanoparticles and (B) PVDF-Fe_3O_4 films.

TABLE III
Magnetization Values of Iron Oxide and the Composite Films

Sample	Magnetic saturation (Ms) (emu/g)	Remnance (Mr) (emu/g)	Coercivity (Hc) Oe
Iron oxide	74.50	6.40	82.0
PF1	1.571	0.10	83.0
PF2	5.563	0.32	82.2
PF3	8.390	0.49	80.4

saturation magnetization (Ms), the remnant magnetization (Mr), and the coercive force (Hc) were determined (Table III). Ms, Mr, and Hc of iron oxide nanoparticles are 74.50 emu/g, 6.4 emu/g, and 82 Oe, respectively. This reveals the ferromagnetic nature of the nanoparticles. As expected the magnetization of PVDF–magnetite composites are comparatively lower. This is mainly because Fe_3O_4 nanoparticles are embedded into a nonmagnetic polymer matrix.[19–22] With the increase in the magnetic content Ms value of the composite also increases. These results suggest that ferromagnetic behavior observed in the composites arose from the magnetic Fe_3O_4 nanoparticles. Xu et al. have also observed similar trend and have attributed this to the increasing tendency of the nanoparticles to aggregate on increasing their content.[8] The prepared magnetic composite films can be further exploited for electromagnetic applications.

CONCLUSIONS

In summary, Fe_3O_4 nanoparticles synthesized by the hydrothermal method, were used to prepare the PVDF-magnetite composite films by spin coating technique. The SEM micrographs of the composite films showed the increasing aggregation of Fe_3O_4 nanoparticles on the surface and inside of the porous PVDF matrix. DSC analysis of the membranes indicated that the interaction between Fe_3O_4 and PVDF as well as the extrusion effect of Fe_3O_4 content decreased the crystalline phase. The conductivity and the magnetization of the composite films was strongly influenced by the Fe_3O_4 content. The conductivity increased with increase in Fe_3O_4 content with a value of 6.52 S/cm for 5 wt % content in the composite film. Also the Fe_3O_4 nanoparticles rendered the PVDF polymer magnetic, the magnetization increasing with increase in the Fe_3O_4 content. A combination of both conducting and magnetic components can be successfully used for electromagnetic applications.

The authors gratefully acknowledge DST, India for their financial support in the form of an R&D project grant. They also like to thank Mr. Sivakumar, Indian Insitute of Technology, Kanpur for helping us with magnetic measurements. ASB is thankful to NITK Surathkal for the award of a research fellowship.

References

1. Prinz, G. A. Science 1998, 282, 1660.
2. Iwauchi, K. Jpn J Appl Phys 1971, 10, 1520.
3. Yan, L.; Li, Y. S.; Xiang, C. B.; Xianda, S. J Membr Sci 2006, 276, 162.
4. Qureshi, A.; Aitindal, A.; Mergen, A. Sens Actuators B 2009, 138, 71.
5. Slama, J.; Dosoudil, R.; Vicen, R.; Gruskova, A.; Olah, V.; Hudec, I.; Usak, E. J Magn Magn Mater 2003, 254, 195.
6. Lebourgeois, R.; Berenguer, S.; Ramiarinjaona, C.; Waeckerle, T. J Magn Magn Mater 2003, 254, 191.
7. Paterson, J. H.; Devine, R.; Phelps, A. D. R. J Magn Magn Mater 1999, 196, 394.
8. Xu, C.; Ouyang, C.; Jia, R.; Li, Y.; Wang, X. J Appl Polym Sci 2009, 111, 1763.
9. Yin, M.; Willis, A.; Redl, F.; Turro, N. J.; O'brien, S. P. J Mater Res 2004, 19, 1208.
10. Wunderlich, B. Macromolecular Physics, 3rd ed.; Academic Press: New York, 1980; p 50.
11. Wang, Y.-J.; Kim, D. Electrochim Acta 2007, 52, 3181.
12. Croce, F.; Appetecchi, G. B.; Persi, L.; Scrosati, B. Nature 1998, 394, 456.
13. Wang, G.; Roos, J.; Brinkmann, D.; Capuano, F.; Croce, F.; Scrosati, B. Solid State Ionics 1992, 53, 1102.
14. Chu, P. P.; Reddy, M. J. J Power Sources 2003, 115, 288.
15. Weston, J. E.; Steele, B. C. H. Solid State Ionics 1982, 7, 75.
16. Wieczorek, W.; Such, K.; Wycilik, H.; Pocharski, J. Solid State Ionics 1989, 36, 255.
17. Kumar, B.; Rodrigues, S. J. J Electrochem Soc 2001, 148, A1336.
18. Liu, Y.; Lee, J. Y.; Hong, L. J Appl Polym Sci 2003, 89, 2815.
19. Yang, J.; Park, S. B.; Yoon, H. G.; Huh, Y. M.; Haam, S. Int J Pharm 2006, 324, 185.
20. Cui, L.; Gu, H.; Xu, H.; Shi, D. Mater Lett 2006, 60, 2929.
21. Pelecky, D. L. L.; Rieke, R. D. Chem Mater 1996, 8, 1770.
22. Jacobo, S. E.; Aphesteguy, J. C.; Anton, R. L.; Schegoleva, N. N.; Kurlyandskaya, G. V. Eur Polym J 2007, 43, 1333.